Aligning Scan Locations from Consecutive Spectral-Domain Optical Coherence Tomography Examinations: A Comparison among Different Strategies

Andrea Giani,[1] *Marco Pellegrini,*[1] *Alessandro Invernizzi, Mario Cigada, and Giovanni Staurenghi*

Purpose. We compared intrasession repeatability values produced by different spectral-domain optical coherence tomography (SD-OCT) instruments when measuring macular retinal thickness from consecutive examinations.

Methods. A total of 40 eyes from 23 healthy subjects and 47 eyes from 42 patients with macular edema were enrolled in the study. Subjects underwent two consecutive SD-OCT examinations using three instruments: Spectralis HRA+OCT, Cirrus, and RS 3000. For the second SD-OCT examination, the scan location was aligned to the baseline exam using different strategies: RS 3000 eye-tracking (pre-acquisition), Spectralis follow-up (during acquisition), Cirrus fovea finding (postacquisition), and Cirrus macular change analysis (postacquisition). Macular retinal thickness values from the consecutive examinations were evaluated to assess repeatability of the measurements.

Results. In healthy subjects all of the strategies used for scan location alignment for the second examination provided good repeatability. For instance, intraclass correlation coefficients (ICC) from the central subfield were between 0.88 (RS 3000 eye-tracking) and 0.99 (Spectralis follow-up). In subjects affected by macular edema, the results were excellent. Cirrus macular change analysis and Spectralis follow-up produced ICC values equaled 1.00 in the central subfield. Cirrus fovea finding and RS 3000 eye-tracking produced slightly lower ICC values (0.98 and 0.99, respectively) in the central subfield.

Conclusions. All of the strategies for aligning consecutive SD-OCT scan locations produced repeatable retinal thickness values. The best results were obtained using the Spectralis with follow-up and Cirrus with macular change analysis. (*Invest Ophthalmol Vis Sci.* 2012;53:7637–7643) DOI:10.1167/iovs.12-10047

From the Eye Clinic, Department of Clinical Science "Luigi Sacco," Luigi Sacco Hospital, University of Milan, Milan, Italy.

[1]These authors contributed equally to the work presented here and should therefore be regarded as equivalent authors.

Presented in part at the Association for Research in Vision and Ophthalmology Annual Meeting, Fort Lauderdale, Florida, May 2010.

Supported by research grants from Zeiss Meditec to The Sacco Hospital Eye Clinic (not inherent to this work) and from Nidek, Inc. (provision of the instrument tested in this work).

Submitted for publication April 18, 2012; revised August 16 and October 16, 2012; accepted October 21, 2012.

Disclosure: **A. Giani**, None; **M. Pellegrini**, None; **A. Invernizzi**, None; **M. Cigada**, None; **G. Staurenghi**, Nidek, Inc. (F), Heidelberg Engineering (C), Zeiss Meditec (R)

Corresponding author: Giovanni Staurenghi, Eye Clinic, Luigi Sacco Hospital, University of Milan, Via G.B. Grassi, 74 - 20157 Milano, Italy; giovanni.staurenghi@unimi.it.

Spectral-domain optical coherence tomography (SD-OCT) is a fundamental tool for clinical practice in ophthalmology.[1–3] Its ability to resolve retinal layers accurately allows a precise evaluation of several pathologies that affect the macula,[4–6] and retinal thickness can be assessed and compared between consecutive visits.[7,8] Moreover, the thickness of the retinal nerve fiber layer (RNFL), which is reduced in glaucoma, can be measured and evaluated over time.[9,10] This ability to measure retina and RNFL thickness has revolutionized the approach for evaluating treatments. For instance, clinical trials in exudative age-related macular degeneration (AMD) and in diabetic macular edema use SD-OCT to assess variations in macular thickness as one of the outcome measures.[11,12] Therefore, the ability to repeat consecutive scans precisely in the same retinal position becomes essential. Different SD-OCT instruments use various strategies to achieve this goal, basically by using eye-tracking systems or software re-elaboration.[13] The latter method generally is based upon the identification of landmarks, such as the fovea or retinal vessels, and consecutive image transformation. In our study, we evaluated these different approaches and we compared repeatability values among instruments.

Methods

Our prospective study was performed on consecutive subjects at the Eye Clinic, Department of Clinical Science, Luigi Sacco Hospital, University of Milan, after obtaining informed written consent. The study was approved by the local institutional review board and adhered to the tenets of the Declaration of Helsinki. The study was conducted on healthy volunteers with normal retinas, and on patients affected by macular edema caused by exudative AMD, diabetic retinopathy, or retinal vein occlusion. Subjects with insufficient transparency of the ocular media were excluded. All enrolled subjects underwent consecutive SD-OCT examinations on the same clinic visit using three different SD-OCT instruments: Cirrus (software version 5.0.0.326; Carl Zeiss Meditec Inc., Dublin, CA), Spectralis HRA+OCT (software version Eye Explorer 1.6.4.0; Heidelberg Engineering, Heidelberg, Germany), and Nidek RS 3000 (software version NAVIS EX 1.1.0.0; Nidek Co. Ltd., Gamagori, Japan).

The order of examination by the different SD-OCT instruments and protocols was chosen randomly for each subject. Between the initial baseline imaging and the follow-up re-imaging to determine the repeatability for each instrument, there was at least a 5-minute rest period. For each machine, the best achievable image quality was obtained by providing artificial tears/lubricants before each scanning session and accounting for the best-corrected visual acuity when adjusting the focus. Minimum scan quality was 5 (quality score provided by the software, range 0–10) for Cirrus (Carl Zeiss Meditec Inc.) and RS 3000 (Nidek Co. Ltd.), and $\geq$20 decibels (dB) for Spectralis (Heidelberg Engineering). After each examination, the images were deemed acceptable if the retina was clearly visible and distinguishable, and the full depth and extent of the retina was visualized in every B-

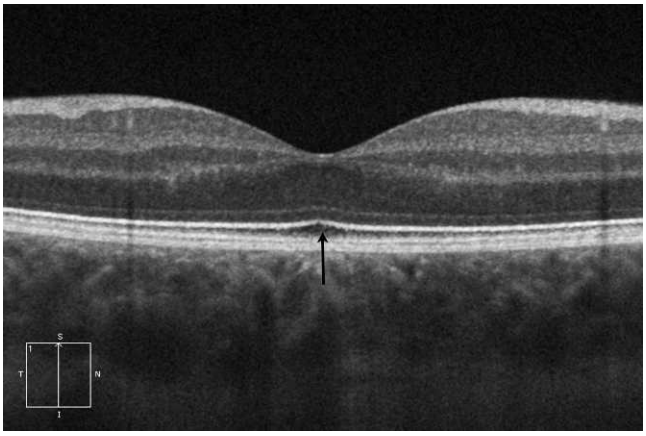

Figure 1. SD-OCT images illustrating the Zeiss Cirrus fovea finding rationale. The software is able to identify a subfoveal area with decreased reflectivity between the interface of the inner/outer photoreceptor segments and the retinal pigment epithelium (*black arrow*).

scan. Images with eye movement or blinking artifacts were excluded from analysis.

SD-OCT Protocols

Standard analysis protocols for macular examination were used for each single instrument. For Cirrus (Carl Zeiss Meditec Inc.), we used the "Macular Cube" protocol that imaged a 6×6 mm area with 128 raster B-scans, each composed of 512 A-scans. For Spectralis (Heidelberg Engineering), we used the "Fast" protocol that imaged a $20° \times 20°$ area with 9 raster B-scans, each composed of 768 A-scans and resulting from an average of 9 frames. For the RS 3000 (Nidek Co. Ltd.), we used the "Macula Map" protocol that imaged a 6×6 mm area with 64 raster B-scans, each composed of 1024 A-scans.

Four different strategies for aligning follow-up images were tested in our study:

1. Pre-acquisition strategy: RS 3000 (Nidek Co. Ltd.) eye tracking. The RS 3000 (Nidek Co. Ltd.) relied on a pre-acquisition eye tracking system. Retinal vessels of the baseline scanning laser ophthalmoscope (SLO) image allowed the device to position the current scan pattern correctly. When the two SLO images were aligned perfectly, the new scan was acquired with no active tracking of eye movements during the acquisition procedure.
2. During acquisition strategy: Spectralis (Heidelberg Engineering) follow-up. The Spectralis (Heidelberg Engineering) combined SD-OCT technology with a confocal scanning laser ophthalmoscope (cSLO). At the baseline examination, each SD-OCT B-scan was registered and locked to a cSLO reference image. In the following examination, during the acquisition of the images, SD-OCT software identified previous scan locations on the cSLO reference image. With an active eye-tracking system, the software guided the SD-OCT laser to scan the same location again.
3. Postacquisition strategy: Cirrus (Carl Zeiss Meditec Inc.) fovea finding. The Cirrus software (Carl Zeiss Meditec Inc.) attempted to identify an area with decreased reflectivity below the internal limiting membrane (Fig. 1). This area usually was located under the fovea, where the inner layers of the retina came together, and the dark Henle fiber and outer nuclear layer came upward. Because this method was independent of the foveal pit, it still was reliable in cases of macular edema.
4. Postacquisition strategy: Cirrus (Carl Zeiss Meditec Inc.) macular change analysis. The Cirrus (Carl Zeiss Meditec Inc.) macular change analysis allowed alignment and comparison of SD-OCT scans from consecutive exams. The registration was based on detecting the vessel landmarks automatically from the corresponding SD-OCT images and aligning them accurately. The algorithm used a rigid transformation model that corrects for x,y translations as well as rotation between the two scans.

Table 1. Evaluation of Repeatability of Retinal Thickness Measurements with Different Analysis Protocol in Healthy Subjects

	MRT	LOA	ICC	COV
Central				
Cirrus FF	264 ± 14	−6, 6	0.97 (0.95)	0.59 ± 0.60
Cirrus MCA	264 ± 13	−9, 7	0.95 (0.91)	0.77 ± 0.81
Spectralis FU	288 ± 13	−5, 4	0.99 (0.98)	0.37 ± 0.41
RS 3000 ET	277 ± 14	−15, 12	0.88 (0.78)	1.16 ± 1.28
Parafovea superior				
Cirrus FF	331 ± 17	−12, 12	0.94 (0.90)	0.74 ± 1.06
Cirrus MCA	331 ± 17	−12, 14	0.93 (0.87)	0.82 ± 1.23
Spectralis FU	358 ± 25	−2, 2	1.00 (1.00)	0.17 ± 0.16
RS 3000 ET	352 ± 23	−29, 34	0.66 (0.44)	0.87 ± 2.79
Parafovea temporal				
Cirrus FF	317 ± 14	−7, 8	0.96 (0.93)	0.59 ± 0.60
Cirrus MCA	316 ± 14	−8, 7	0.96 (0.93)	0.62 ± 0.58
Spectralis FU	344 ± 15	−3, 3	1.00 (0.99)	0.23 ± 0.24
RS 3000 ET	334 ± 15	−4, 6	0.98 (0.97)	0.37 ± 0.42
Parafovea nasal				
Cirrus FF	334 ± 17	−7, 8	0.98 (0.96)	0.62 ± 0.51
Cirrus MCA	334 ± 17	−9, 8	0.97 (0.95)	0.71 ± 0.55
Spectralis FU	363 ± 18	−4, 4	1.00 (0.99)	0.28 ± 0.31
RS 3000 ET	349 ± 17	−7, 7	0.98 (0.96)	0.49 ± 0.50
Parafovea inferior				
Cirrus FF	328 ± 17	−9, 9	0.97 (0.94)	0.64 ± 0.66
Cirrus MCA	328 ± 17	−8, 9	0.97 (0.94)	0.62 ± 0.68
Spectralis FU	356 ± 18	−2, 3	1.00 (1.00)	0.21 ± 0.20
RS 3000 ET	343 ± 17	−8, 9	0.97 (0.94)	0.56 ± 0.73
Perifovea superior				
Cirrus FF	288 ± 15	−8, 6	0.97 (0.92)	0.70 ± 0.55
Cirrus MCA	287 ± 15	−7, 9	0.97 (0.90)	1.10 ± 1.55
Spectralis FU	310 ± 12	−4, 4	0.99 (0.99)	0.33 ± 0.28
RS 3000 ET	n.a.			
Perifovea temporal				
Cirrus FF	265 ± 12	−8, 12	0.91 (0.77)	1.00 ± 0.97
Cirrus MCA	265 ± 12	−7, 8	0.95 (0.86)	0.75 ± 0.68
Spectralis FU	293 ± 12	−2, 3	0.99 (0.99)	0.25 ± 0.24
RS 3000 ET	n.a.			
Perifovea nasal				
Cirrus FF	305 ± 17	−5, 5	0.99 (0.97)	0.43 ± 0.38
Cirrus MCA	305 ± 17	−5, 6	0.99 (0.96)	0.70 ± 0.99
Spectralis FU	326 ± 16	−4, 3	0.99 (0.99)	0.29 ± 0.26
RS 3000 ET	n.a.			
Perifovea inferior				
Cirrus FF	278 ± 14	−8, 13	0.91 (0.73)	1.08 ± 1.10
Cirrus MCA	278 ± 14	−9, 10	0.95 (0.85)	0.75 ± 0.68
Spectralis FU	299 ± 15	−7, 8	0.97 (0.94)	0.47 ± 0.68
RS 3000 ET	n.a.			

No statistical significant differences were found ($P > 0.05$ in all the analyses). MRT, mean retinal thickness (μm); FF, fovea finding; MCA, macular change analysis; ET, eye tracking; FU, follow-up; n.a., not available (due to loss of data).

Because the Cirrus (Carl Zeiss Meditec Inc.) used two different strategies for aligning consecutive images, the patients underwent four exams with this instrument: a baseline examination followed by re-examination with fovea finding, and then another baseline examination followed by the macula change analysis. For the Spectralis (Heidelberg Engineering) and RS 3000 instruments (Nidek Co. Ltd.), the patients

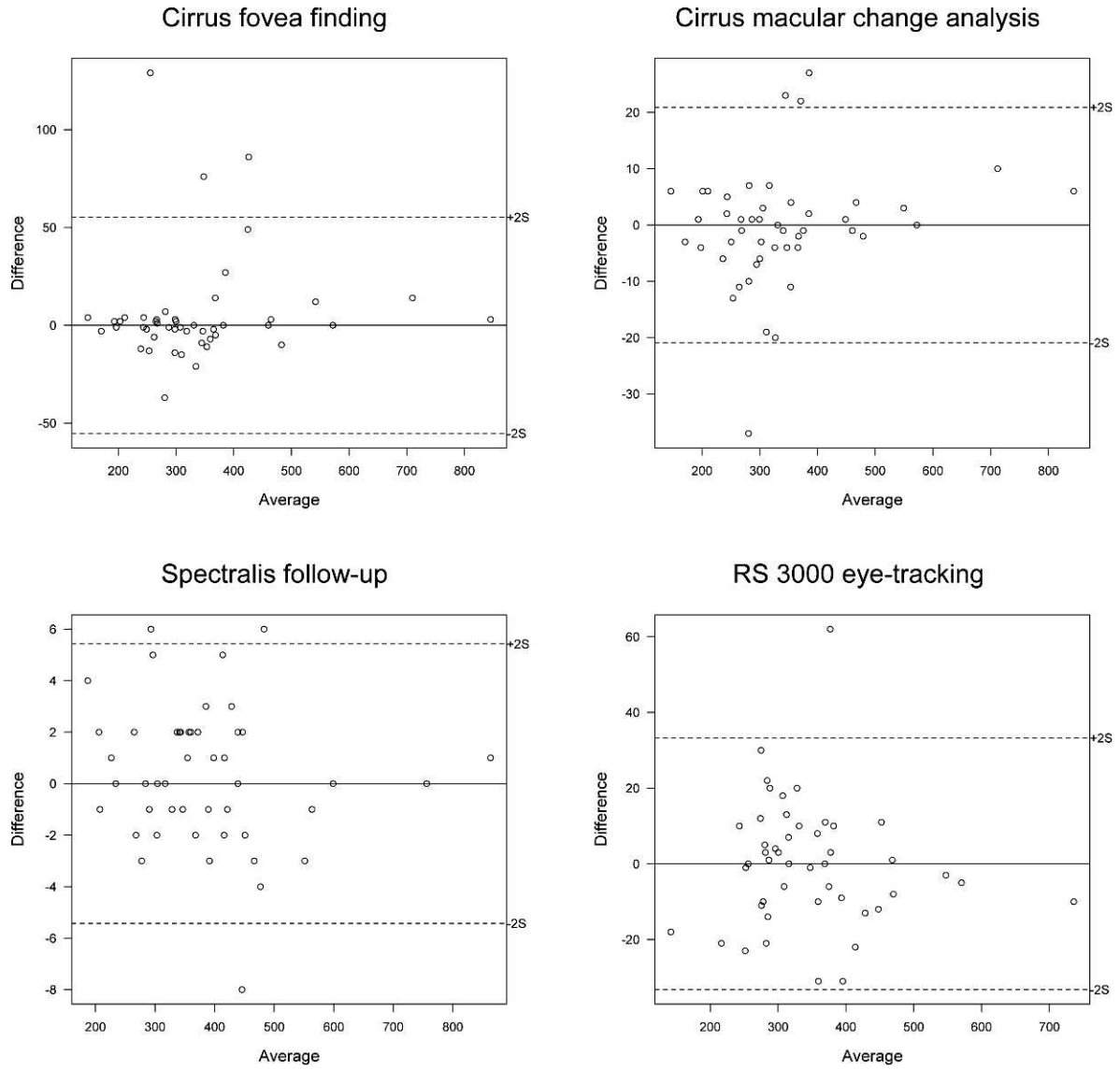

Figure 2. Bland-Altman graphs from the analysis in healthy subjects. All of the strategies for scan location alignment produced narrow limits of agreement. No proportional bias was evident.

underwent a baseline examination followed by eye-tracker guided re-examination. For each patient, all of the baseline and re-imaging exams were conducted during a single office visit.

Data Analysis

All of the instruments provided a retinal thickness map based on the early treatment diabetic retinopathy study (ETDRS) model. For each instrument, the diameter of each area was 1, 3, and 6 mm. The peripheral concentric areas were divided into 8 subfields: superior, inferior, nasal, and temporal for parafoveal (3 mm) and perifoveal (6 mm) subfields. For each one of these, as well as for the central area, the software elaborated the mean value from all of the thickness measurements on each single A-scan within the imaged areas. In our study, the comparative analysis was assessed on the mean thickness values of the analyzed subfields.

R language statistics software (available online at http://www.R-project.org. Last accessed February 12, 2012) was used. Repeated measurements for each instrument were analyzed using Bland-Altman analysis, setting the limits of agreement (LOA) to two SDs. Additionally, the intraclass correlation coefficients (ICC, single random users form) were calculated. Finally, the coefficient of variation (COV), defined as the ratio of the SD and the mean of the differences between the two repeated measures, was calculated.

Results

A total of 90 eyes from 65 subjects was enrolled in the study. Three eyes were excluded because of poor fixation ($n = 1$) or poor measurement quality due to cataract ($n = 2$). In these conditions all three systems failed to produce acceptable examinations. A loss of data occurred for the perifoveal subfields with the RS 3000 (Nidek Co. Ltd.).

Healthy Subjects

A total of 40 eyes from 23 subjects with normal retinas was enrolled in the analysis. There were 12 male and 11 female subjects (mean age 36.6 years, range 26–61 years). The mean best corrected visual acuity measured with ETDRS charts was 20/20 (range 20/20–20/16).

Table 2. Evaluation of Repeatability of Retinal Thickness Measurements with Different Analysis Protocol in Subjects with Cystoid Macular Edema

	MRT	LOA	ICC	COV
Central				
Cirrus FF	340 ± 133	−48, 60	0.98 (0.96)	2.93 ± 5.91
Cirrus MCA	338 ± 132	−21, 20	1.00 (1.00)	1.58 ± 1.79
Spectralis FU	385 ± 130	−5, 6	1.00 (1.00)	0.42 ± 0.37
RS 3000 ET	346 ± 101	−33, 33	0.99 (0.98)	2.73 ± 2.60
Parafovea superior				
Cirrus FF	343 ± 76	−51, 62	0.98 (0.96)	2.47 ± 4.13
Cirrus MCA	344 ± 76	−20, 21	1.00 (0.98)	1.07 ± 1.67
Spectralis FU	369 ± 84	−6, 7	1.00 (1.00)	0.44 ± 0.43
RS 3000 ET	346 ± 61	−27, 23	0.98 (0.96)	1.49 ± 2.21
Parafovea temporal				
Cirrus FF	348 ± 84	−34, 33	0.98 (0.97)	1.54 ± 2.79
Cirrus MCA	349 ± 89	−12, 14	1.00 (1.00)	0.83 ± 1.03
Spectralis FU	368 ± 92	−6, 7	1.00 (1.00)	0.45 ± 0.46
RS 3000 ET	345 ± 77	−29, 26	0.95 (0.92)	1.77 ± 2.39
Parafovea nasal				
Cirrus FF	353 ± 79	−33, 27	0.97 (0.95)	1.60 ± 2.93
Cirrus MCA	349 ± 82	−21, 19	1.00 (0.99)	1.00 ± 1.50
Spectralis FU	387 ± 80	−9, 8	1.00 (1.00)	0.55 ± 0.67
RS 3000 ET	354 ± 65	−28, 19	0.98 (0.96)	1.54 ± 2.55
Parafovea inferior				
Cirrus FF	348 ± 84	−33, 36	0.98 (0.97)	1.41 ± 2.87
Cirrus MCA	347 ± 81	−7, 8	1.00 (1.00)	0.61 ± 0.53
Spectralis FU	370 ± 78	−11, 10	1.00 (1.00)	0.63 ± 0.99
RS 3000 ET	342 ± 71	−85, 74	0.84 (0.73)	3.10 ± 6.92
Perifovea superior				
Cirrus FF	288 ± 44	−18, 16	0.98 (0.97)	1.19 ± 1.58
Cirrus MCA	287 ± 44	−18, 21	0.97 (0.95)	1.11 ± 2.66
Spectralis FU	306 ± 49	−4, 4	1.00 (1.00)	0.39 ± 0.36
RS 3000 ET	n.a.			
Perifovea temporal				
Cirrus FF	277 ± 58	−25, 22	0.98 (0.96)	1.39 ± 2.57
Cirrus MCA	279 ± 60	−15, 15	0.95 (0.98)	0.99 ± 1.72
Spectralis FU	293 ± 57	−7, 5	1.00 (1.00)	0.38 ± 0.64
RS 3000 ET	n.a.			
Perifovea nasal				
Cirrus FF	312 ± 49	−9, 11	0.99 (0.99)	0.72 ± 0.86
Cirrus MCA	318 ± 61	−9, 11	1.00 (0.99)	0.65 ± 0.90
Spectralis FU	331 ± 46	−8, 8	1.00 (0.99)	0.44 ± 0.72
RS 3000 ET	n.a.			
Perifovea inferior				
Cirrus FF	283 ± 51	−42, 43	0.92 (0.85)	2.10 ± 4.89
Cirrus MCA	288 ± 52	−7, 9	1.00 (0.99)	0.76 ± 0.61
Spectralis FU	303 ± 49	−15, 17	0.99 (0.97)	0.81 ± 1.83
RS 3000 ET	n.a.			

No statistical significant differences were found ($P > 0.05$ in all the analyses).

In the central subfield, the mean baseline examination retinal thickness varied from 264 ± 14 μm for the Cirrus (Carl Zeiss Meditec Inc.) using fovea finding to 288 ± 13 μm for the Spectralis (Heidelberg Engineering) (Table 1). The Bland-Altman analysis showed very narrow LOAs for the Spectralis (Heidelberg Engineering) in all analyzed sectors. In the central subfield, the LOAs were −5 to 4 μm. Also, the Cirrus (Carl Zeiss Meditec Inc.) had narrow LOAs in all sectors, with no evident difference between the fovea finding and the macular change analysis. In the central subfield, the LOAs were −6 to 6 μm when using the fovea finding and −9 to 7 μm when using the macular change analysis. The RS 3000 (Nidek Co. Ltd.) with eye tracking had higher LOAs in the central (−15 to 12 μm) and superior (−29 to 34 μm) subfields, while the other values were comparable to the ones found with the Cirrus (Carl Zeiss Meditec Inc.). The ICC test and COV values confirmed these results. In particular, the Spectralis (Heidelberg Engineering) had the highest ICC values and the lowest COVs in all of the analyzed sectors. In the central sector, the ICC was 0.99, while the COV was 0.37 ± 0.41. The Bland-Altman graphs did not reveal any proportional bias of measurements (Fig. 2).

Macular Edema Patients

A total of 47 eyes from 42 patients affected by macular edema was enrolled in the analysis. There were 21 male and 18 female subjects (mean age 71.1 years, range 40–86 years). The mean best corrected visual acuity measured with ETDRS charts was 20/50 (range 20/200–20/20). Among the eyes, 60% (28/47) had exudative AMD, 34% (16/47) had diabetic macular edema, and the remaining 6% (3/47) had central vein occlusion.

In the central subfield, the mean baseline examination retinal thickness varied from 340 ± 133 μm as measured by the Cirrus (Carl Zeiss Meditec Inc.) using fovea finding to 385 ± 130 μm for the Spectralis (Heidelberg Engineering) (Table 2). The Bland-Altman analysis showed very narrow LOAs for the Spectralis (Heidelberg Engineering) in all of the sectors. In the central subfield, the LOAs were −5 to 6 μm. For the Cirrus (Carl Zeiss Meditec Inc.), the central subfield LOAs were −21 to 20 μm for the macular change analysis, and slightly higher, −48 to 60 μm, for the fovea finding. For the RS 3000 (Nidek Co. Ltd.), the central subfield LOAs were −33 to 33 μm. The Spectralis (Heidelberg Engineering) and Cirrus (Carl Zeiss Meditec Inc.) with macular change analysis produced ICC values of 1.00 in the central sector. The Cirrus (Carl Zeiss Meditec Inc.) with fovea finding and the RS 3000 (Nidek Co. Ltd.) had slightly lower central sector ICCs, 0.98 and 0.99, respectively. The central subfield COV values confirmed that Spectralis (Heidelberg Engineering) and Cirrus (Carl Zeiss Meditec Inc.) with macular change analysis produced the best results, 0.42 ± 0.37 and 1.58 ± 1.79, respectively. For the Cirrus (Carl Zeiss Meditec Inc.) with fovea finding and the RS 3000 (Nidek Co. Ltd.), the COV values were 2.93 ± 5.91 and 2.73 ± 2.60, respectively. The Bland-Altman graphs did not reveal any proportional bias of measurements (Fig. 3).

Discussion

In our study we evaluated different systems used by SD-OCT instruments to align consecutive evaluations. We found that all of these systems produced good results in terms of repeatability. In normal and pathologic conditions, the Bland-Altman LOAs always were narrow. In the vast majority of cases, the ICC values were close to 1.00, which represents a perfect agreement between two repeated measurements. Among the different systems, we found the real-time eye tracker used by Spectralis (Heidelberg Engineering) produced very good results. This finding was expected because the real-time eye tracker is able to couple the SD-OCT location to cSLO images.[14] This during acquisition strategy allows continuous alignment of the SD-OCT position at the correct location. In the follow-up modality, this system permits precise positioning of the SD-OCT scans in the same location during consecutive visits. This unique feature provides excellent repeatability in the measurements of macular and RNFL thicknesses.[13–17] In glaucoma, this is extremely useful, since the correlation between the

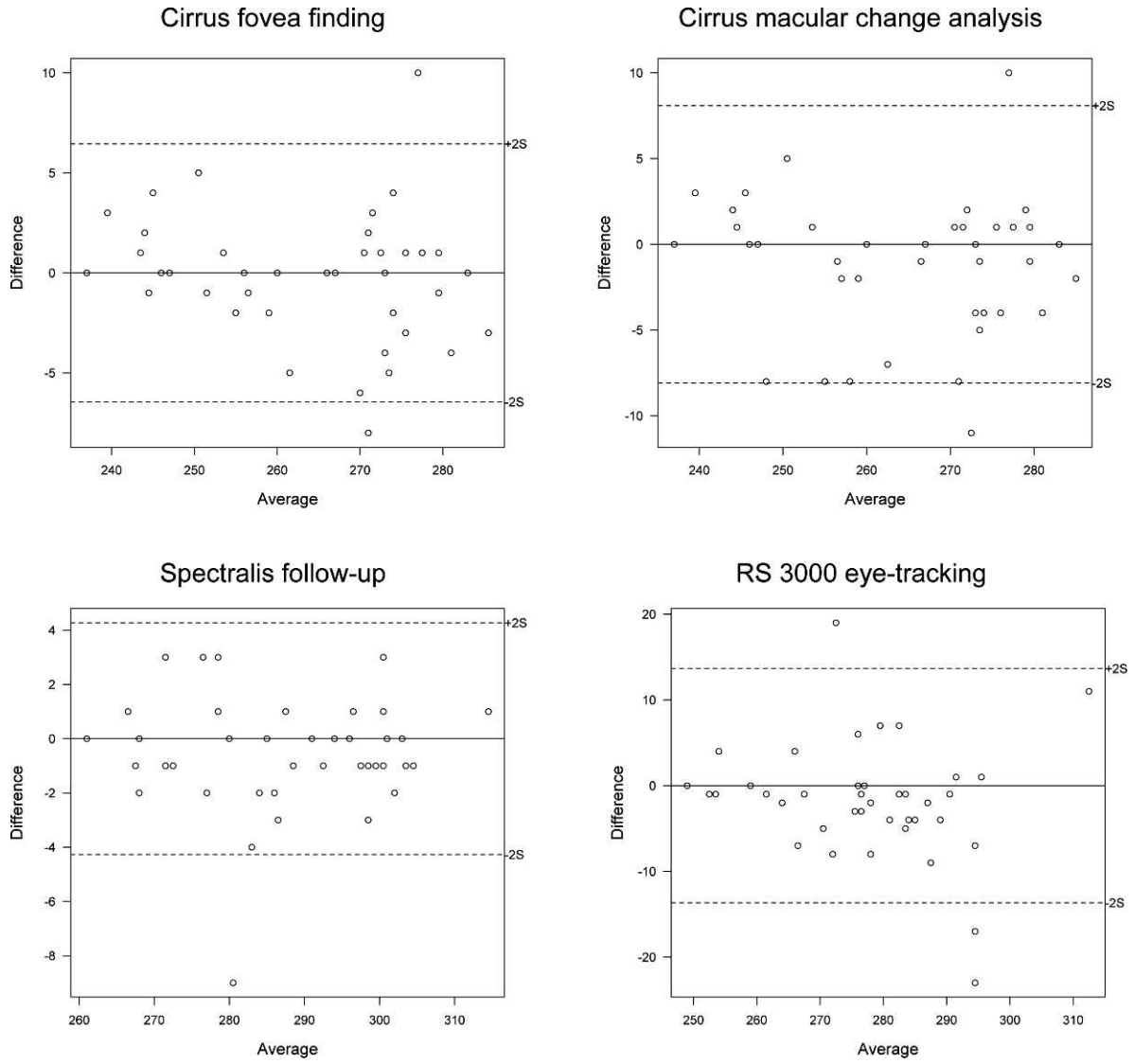

Figure 3. Bland-Altman graphs from the analysis in patients with macular edema. Despite abnormalities of retinal architecture, the limits of agreement were narrow. No proportional bias was evident.

progression of the pathology and RNFL thinning is well documented. Moreover, thinning of RFNL may precede the loss of visual field function.[13] In our study, the follow-up function of the Spectralis (Heidelberg Engineering) was not influenced by the presence of macular edema, thus providing good reproducibility even in pathologic cases.

Compared to the strategy applied by the Spectralis (Heidelberg Engineering), the Cirrus (Carl Zeiss Meditec Inc.) and RS 3000 (Nidek Co. Ltd.) use different approaches. In particular, the Cirrus (Carl Zeiss Meditec Inc.) uses a postacquisition strategy. With the fovea finding modality, the software attempts to identify the location of the fovea. Instead of identifying the fovea depression, which usually is absent in cases of macular edema, the system searches for a hyporeflective area located normally in the outer photoreceptor segments under the fovea. In macular change analysis modality, the Cirrus aligns the SLO images from consecutive visits, and then adjusts the position of SD-OCT lines accordingly. In our study these different approaches showed similar results when measuring normal retinas, and they were only slightly worse than the Spectralis (Heidelberg Engineering). When measuring retinal thickness in eyes affected by macular edema, the Cirrus (Carl Zeiss Meditec Inc.) with fovea finding produced slightly worse results. This finding was not unexpected because in macular edema the visualization of the outer retinal layers may be reduced. In particular the identification of the interface between outer and inner segments of photoreceptors sometimes is challenging. This leads to a less accurate localization of the subfoveal hyporeflective area in these cases. Thus, the fovea finding approach may become less precise and provide less reproducibility. On the other hand, with the macular change analysis the system is not affected by reduced retinal visualization, and the reproducibility results were excellent. Theoretically, this strategy may fail when vessels recognition is impaired, for example in case of severe intraretinal hemorrhages, or when the infrared image is not of sufficient quality. However, within the cases included in our study, the system never failed in achieving images alignment. In summary, the fovea finding can produce good results when retinal disruption is mild, or when the alterations are external to the fovea region. The macular change analysis appears to be more precise in more severe foveal disruption, but requires good quality of the infrared image.

Lastly, the RS 3000 (Nidek Co. Ltd.) uses a pre-acquisition strategy. The eye tracker of the instrument couples the SD-OCT position to the SLO image before the acquisition starts. For follow-up imaging, the SD-OCT scan is aligned precisely to the previous visit position. During acquisition the tracker does not correct for eye movements. Thus, the system relies on the fixation of the patient and the ability to keep the sight as steady as possible during acquisition. In our study, this approach produced good reproducibility results in subjects with normal retinas. In eyes affected by cystoid macular edema, the values were good, but slightly worse compared to other approaches. The most likely explanation of this finding is that these subjects had a reduced ability to fixate. This may have induced broader and more frequent eye movements during acquisition, with consequent loss of alignment.

Previous studies evaluated different instruments' capability of accurately repeating retinal thickness measurements.[16–19] Reproducibility of Spectralis (Heidelberg Engineering) with active eye-tracking was assessed in normal retinas.[16,17] The investigators found COV values in the central subfield to be equal to 0.53,[16] and 0.46,[17] which is in accordance with our findings (0.37 ± 41). Forooghian et al. evaluated Cirrus (Carl Zeiss Meditec Inc.) intrasession repeatability in retinas with diabetic macular edema.[18] They found COV values in the central subfield equal to 2.42 ± 2.43. This result is similar to what we found when using the fovea finding (2.93 ± 5.91), while with the macular change analysis we obtained lower values (1.58 ± 1.79). Ho et al. assessed intrasession repeatability of Cirrus (Carl Zeiss Meditec Inc.) in subjects affected by different pathologies, including cystoid macular edema and retinal degenerations.[19] They found Bland-Altman limits of agreement in the central subfield to range from −184 to 142 μm, and an ICC value equal to 0.92. In our study, we found narrower Bland-Altman limits of agreement, especially when using the macular change analysis (−21 to 20 μm). Moreover, the ICC value from our study was higher (1.00). These results may be explained with the use of postacquisition alignment function, or with the different composition of the study population.

While the Spectralis' (Heidelberg Engineering) approach of active eye-tracking during acquisition provides very high reproducibility values, this approach requires a considerable amount of time. Decisions about the protocol to be used, in terms of scan width and B-scan density, cannot exempt consideration about the time required to acquire images. This is true especially in the elderly and/or subjects with lacrimal dysfunction. The Cirrus (Carl Zeiss Meditec Inc.) and RS 3000 (Nidek Co. Ltd.) alignment strategies require less time and allow performance of swept scans. This means that high-density B-scan protocols for relatively large areas may be employed.[13,16] However, as suggested by others, it is possible that this results in slightly reduced reproducibility,[16] with increasing differences especially over time in repeated visits.[13] This may be true particularly when pathology modifies the retinal structures used for images alignment. Moreover, in pathologies that often are characterized by slight changes in retinal structures over time, this may reduce the reliability of the analysis. The thinning of RNFL may correspond to few micrometers during the follow-up of months or years. In retinal degenerations the atrophy of photoreceptors generally produces minimal changes in the outer retinal layers over time. Therefore, to quantify the evolution of these pathologies efficiently, the analysis must be extremely reliable. Hence, further studies may attempt to test the results that different strategies produce over time in various pathologies.

Another source of variability between consecutive measurements is eye movement. This creates spatial distortions that may affect quantitative analysis and longitudinal assessment of the pathologies. The real-time eye-tracking used by Spectralis (Heidelberg Engineering) is an effective solution for x- and y-axis movements, while z-alignment still requires a software correction.[20] Also, the macular change analysis used by Cirrus (Carl Zeiss Meditec Inc.) may reduce the influence of eye movements, since it is able to re-align images after the acquisition.

In conclusion, our study demonstrates that all the systems used by different SD-OCT instruments to align scan locations from consecutive visits provide good results. Spectralis (Heidelberg Engineering), with active eye-tracking, and Cirrus (Carl Zeiss Meditec Inc.), with macular change analysis, produced the best repeatability.

References

1. Alam S, Zawadzki RJ, Choi S, et al. Clinical application of rapid serial Fourier-domain optical coherence tomography for macular imaging. *Ophthalmology*. 2006;113:1425–1431.
2. Hee MR, Baumal CR, Puliafito CA, et al. Optical coherence tomography of age-related macular degeneration and choroidal neovascularization. *Ophthalmology*. 1996;103:1260–1270.
3. Huang D, Swanson EA, Lin CP, et al. Optical coherence tomography. *Science*. 1991;254:1178–1181.
4. Menke MN, Dabov S, Sturm V. Features of age-related macular degeneration assessed with three-dimensional Fourier-domain optical coherence tomography. *Br J Ophthalmol*. 2008;92:1492–1497.
5. Schuman SG, Koreishi AF, Farsiu S, Jung SH, Izatt JA, Toth CA. Photoreceptor layer thinning over drusen in eyes with age-related macular degeneration imaged in vivo with spectral-domain optical coherence tomography. *Ophthalmology*. 2009;116:488–496.
6. Wojtkowski M, Leitgeb R, Kowalczyk A, Bajraszewski T, Fercher AF. In vivo human retinal imaging by Fourier domain optical coherence tomography. *J Biomed Opt*. 2002;7:457–463.
7. Balk LJ, Sonder JS, Strijbis EM, et al. The physiological variation of the retinal nerve fibre layer thickness and macular volume in humans as assessed by spectral-domain optical coherence tomography. *Invest Ophthalmol Vis Sci*. 2012;53:1241–1257.
8. Bottoni F, De Angelis S, Luccarelli S, Cigada M, Staurenghi G. The dynamic healing process of idiopathic macular holes after surgical repair: a spectral-domain optical coherence tomography study. *Invest Ophthalmol Vis Sci*. 2011;52:4439–4446.
9. Leung CK, Choi N, Weinreb RN, et al. Retinal nerve fiber layer imaging with spectral-domain optical coherence tomography: pattern of RNFL defects in glaucoma. *Ophthalmology*. 2010;117:2337–2344.
10. Leung CK, Liu S, Weinreb RN, et al. Evaluation of retinal nerve fiber layer progression in glaucoma a prospective analysis with neuroretinal rim and visual field progression. *Ophthalmology*. 2011;118:1551–1557.
11. Martin DF, Maguire MG, Ying GS, Grunwald JE, Fine SL, Jaffe GJ. Ranibizumab and bevacizumab for neovascular age-related macular degeneration. *N Engl J Med*. 2011;364:1897–1908.
12. Mitchell P, Bandello F, Schmidt-Erfurth U, et al. The RESTORE study: ranibizumab monotherapy or combined with laser versus laser monotherapy for diabetic macular edema. *Ophthalmology*. 2011;118:615–625.
13. Serbecic N, Beutelspacher SC, Aboul-Enein FC, Kircher K, Reitner A, Schmidt-Erfurth U. Reproducibility of high-resolution optical coherence tomography measurements of the nerve fibre layer with the new Heidelberg Spectralis optical coherence tomography. *Br J Ophthalmol*. 2011;95:804–810.
14. Charbel Issa P, Finger RP, Holz FG, Scholl HP. Multimodal imaging including spectral domain OCT and confocal near infrared reflectance for characterization of outer retinal

pathology in pseudoxanthoma elasticum. *Invest Ophthalmol Vis Sci*. 2009;50:5913–5918.

15. Fleckenstein M, Schmitz-Valckenberg S, Adrion C, et al. Tracking progression with spectral-domain optical coherence tomography in geographic atrophy caused by age-related macular degeneration. *Invest Ophthalmol Vis Sci*. 2010;51: 3846–3852.
16. Menke MN, Dabov S, Knecht P, Sturm V. Reproducibility of retinal thickness measurements in healthy subjects using spectralis optical coherence tomography. *Am J Ophthalmol*. 2009;147:467–472.
17. Wolf-Schnurrbusch UE, Ceklic L, Brinkmann CK, et al. Macular thickness measurements in healthy eyes using six different optical coherence tomography instruments. *Invest Ophthalmol Vis Sci*. 2009;50:3432–3437.
18. Forooghian F, Cukras C, Meyerle CB, Chew EY, Wong WT. Evaluation of time domain and spectral domain optical coherence tomography in the measurement of diabetic macular edema. *Invest Ophthalmol Vis Sci*. 2008;49:4290–4296.
19. Ho J, Sull AC, Vuong LN, et al. Assessment of artifacts and reproducibility across spectral- and time-domain optical coherence tomography devices. *Ophthalmology*. 2009;116: 1960–1970.
20. Xu J, Ishikawa H, Wollstein G, Kagemann L, Schuman JS. Alignment of 3-D optical coherence tomography scans to correct eye movement using a particle filtering. *IEEE Trans. Med. Imaging*. 2012;31:1337–1345.